Deep-Sea Research II 55 (2008) 1348–1359

Contents lists available at ScienceDirect

Deep-Sea Research II

journal homepage: www.elsevier.com/locate/dsr2

Depth-stratified phytoplankton dynamics in Cyclone *Opal*, a subtropical mesoscale eddy

Michael R. Landry [a,*], Susan L. Brown [b], Yoshimi M. Rii [b], Karen E. Selph [b], Robert R. Bidigare [b,c], Eun Jin Yang [d], Melinda P. Simmons [e]

[a] *Scripps Institution of Oceanography, University of California at San Diego, La Jolla, CA 92093-0227, USA*
[b] *Department of Oceanography, University of Hawaii at Manoa, Honolulu, HI 96822, USA*
[c] *Hawaii Institute of Marine Biology, University of Hawaii at Manoa, Honolulu, HI 96822, USA*
[d] *Marine Environment Research Department, Korea Ocean Research & Development Institute, Ansan P.O. Box 29, Seoul 425-600, South Korea*
[e] *Gordon and Betty Moore Foundation, San Francisco, CA 94129-0910, USA*

ARTICLE INFO

Article history:
Accepted 26 February 2008
Available online 5 May 2008

Keywords:
Physical–biological coupling
Prochlorococcus
Diatom bloom
Microzooplankton grazing
Growth rate

ABSTRACT

As part of E-Flux III cruise studies in March 2005, we investigated phytoplankton community dynamics in a cyclonic cold-core eddy (Cyclone *Opal*) in the lee of the Hawaiian Islands. Experimental incubations were conducted under *in situ* temperature and light conditions on a drift array using a two-treatment dilution technique. Taxon-specific estimates of growth, grazing and production rates were obtained from analyses of incubation results based on phytoplankton pigments, flow cytometry and microscopy. Cyclone *Opal* was sampled at a biologically and physically mature state, with an 80–100 m doming of isopycnal surfaces in its central region and a deep biomass maximum of large diatoms. Depth-profile experimentation defined three main zones. The upper (mixed) zone (0–40 m), showed little compositional or biomass response to eddy nutrient enrichment, but growth, grazing and production rates were significantly enhanced in this layer relative to the ambient community outside of the eddy. *Prochlorococcus* spp. dominated the upper mixed layer, accounting for 50–60% of its estimated primary production both inside and outside of *Opal*. In contrast, the deep zone of 70–90 m showed little evidence of growth rate enhancement and was principally defined by a ~100-fold increase of large (>20-μm) diatoms and a shift from *Prochlorococcus* to diatom dominance (~80%) of production. The intermediate layer of 50–60 m marked the transition between the upper and lower extremes but also contained an elevated biomass of physiologically unhealthy diatoms with significantly depressed growth rates and proportionately greater grazing losses relative to diatoms above or below. Microzooplankton grazers consumed 58%, 65% and 55%, respectively, of the production of diatoms, *Prochlorococcus* and the total phytoplankton community in Cyclone *Opal*. The substantial grazing impact on diatoms suggests that efficient recycling was the major primary fate of diatom organic production, consistent with the low export fluxes and selective export of biogenic silica, as empty diatom frustules, in Cyclone *Opal*.

1. Introduction

Although general understanding of open-ocean biogeochemistry and ecology has been greatly advanced by systematic study over the past two decades, there are still major issues—e.g., discrepancies in net system auto- or heterotrophy and nutrient sources for new production—that seem to defy explanation from mean system measurements (e.g., Michaels et al., 1996; McGillicuddy et al., 1998; Karl et al., 2003). Mesoscale eddies, as well as waves and fronts of various kinds, have therefore emerged as mechanisms of interest for explaining pulsed nutrient delivery, cryptic production and flux anomalies at scales that are difficult to extract from classic sampling designs (e.g., McGillicuddy et al., 1999; Siegel et al., 1999; Sakamoto et al., 2004). Eddies, in particular, are common and often long-lived features of ocean circulation with demonstrable, though highly variable, impacts on phytoplankton production, biomass and community structure (Allen et al., 1996; Froneman and Perissinotto, 1996; Tarran et al., 2001; Bidigare et al., 2003; Vaillancourt et al., 2003). Despite these general findings, however, we know very little about the ecology of eddies as perturbed ecosystems, or the comparative dynamics of component populations within their water columns.

The present study was designed to investigate the depth-stratified responses of a subtropical phytoplankton community to strong nutrient perturbation in a cold-core, cyclonic eddy. In effect, the eddy was viewed as a large, relatively well-contained

* Corresponding author. Tel.: +1 858 534 4702; fax: +1 858 534 6500.
E-mail address: mlandry@ucsd.edu (M.R. Landry).

0967-0645/$ - see front matter © 2008 Elsevier Ltd. All rights reserved.
doi:10.1016/j.dsr2.2008.02.001

"patch", not unlike those of open-ocean iron fertilization experiments (Coale et al., 1996; De Baar et al., 2005), except that the limiting nutrients were different and delivered at depth rather than at the surface. In contrast to surface fertilizations, which focus entirely on mixed-layer community responses, deep nutrient delivery was expected to establish varying habitats in the opposing gradients of light and nutrients that might select differently for phytoplankton taxa according to their unique preferences and rate characteristics. The bottom layer was also of special biogeochemical interest since anticipated nutrient enhancements of community size structure and biomass deep in the water column might reasonably translate to more efficient carbon export than production at the surface. Whether this occurs or not depends, however, on the coupling of production, grazing and remineralization processes (Landry et al., 2000b).

Our experiments were conducted in Cyclone *Opal*, a wind-forced, first-baroclinic mode, cold-core eddy that spun up in the lee of the Hawaiian Islands between the islands of Maui and Hawaii and first appeared in satellite imagery on 18 February 2005 (Benitez-Nelson et al., 2007; Dickey et al., 2008). At the time of our study in March, *Opal* was a large mature feature of approximately 4–6 weeks age and 200–220 km diameter that was moving northeast to southwest at a mean translational speed of $\sim$8 km d^{-1}. Isopycnal surfaces (sigma–t = 24.1–24.4 kg m^{-3}) in its central core region of $\sim$30-km diameter had been uplifted 80–100 m relative to surrounding water (Nencioli et al., 2008), and the deep-euphotic zone was dominated by a bloom of large centric diatoms (Brown et al., 2008; Rii et al., 2008). Cyclone *Opal* therefore, represented, quite literally, a natural "bottom-up" forcing of community structure and production of substantial magnitude, and an excellent opportunity to compare the stimulatory impact of the eddy on contrasting phytoplankton assemblages in a stratified water column.

2. Materials and methods

2.1. In situ dilution experiments

In order to study the perturbation responses and dynamics of the microplankton community in Cyclone *Opal* under *in situ* conditions of temperature and light, we designed and scaled our experiments so that they could be incubated attached to a weighted line hanging from a free-drifting surface float. For each array deployment, experimental incubations were conducted as a depth profile spanning the range of the euphotic zone (from 10 m to the depth representing an average of 0.5% of surface illumination, as determined in daytime light profiles from a CTD-mounted PAR sensor; Rii et al., 2008). We conducted five sets of 24-h incubation experiments in the center region of Cyclone *Opal* (IN stations) from 16 to 21 March 2005. For comparative purposes, three additional sets of experiments were conducted from 24 to 26 March at "control" (OUT) stations far removed from the eddy influence.

The basic experimental design followed the two-treatment dilution approach of Landry et al. (1984). For each set of experiments, we collected water at seven depths (from 10 to 90–140 m) and prepared pairs of clear polycarbonate bottles (2.7 or 2.2 L) with whole seawater (100%) and 37% whole seawater (diluted with 0.1-μm filtered seawater) at each depth. Seawater was filtered directly from the Niskin bottles using a peristaltic pump, silicone tubing and an in-line Suporcap filter capsule that had previously been acid washed (10% trace-metal grade HCl followed by Milli-Q and seawater rinses). Dilution treatment bottles received pre-measured volumes of filtered water from the collection depths, then both diluted and whole seawater treatments were gently filled (silicone tubing below the water level) with unscreened water from the Niskin bottles, alternating flow into each bottle until they were both topped off at about the same time. Each bottle was subsampled for flow cytometric (FCM) analysis to confirm initial concentrations and volume dilutions. The bottles were then tightly capped, placed in pairs into net bags and clipped onto attached rings at the depth of collection on the array line during deployment. For back-to-back array deployments, we recovered the initial set of experiments first, placed the bottles and net bags in a dark, seawater-cooled deck incubator, and set-up and deployed the second set of experiments before taking final subsamples from the first set. All experiments were started in the early morning and deployed prior to sunrise, the total elapsed time from Niskin sampling to array deployment taking about 1.5 h.

Samples were taken for pigment, flow cytometry and microscopical analyses at the start and end of each experiment to determine initial abundances and biomass concentrations for component populations and to assess their rates of growth and grazing losses in the dilution incubations. These analyses are further described below.

2.2. HPLC pigment analyses

Phytoplankton pigments were analyzed by high-performance liquid chromatography (HPLC) according to the methods of Bidigare et al. (2005). Sample volumes of 1.7–2.1 L, depending on other subsampling needs, were concentrated onto 25-mm Whatman GF/F glass fiber filters. The filters were wrapped in aluminum foil, frozen in liquid nitrogen and stored at −85 °C until analysis. Pigments were extracted in 3 mL of 100% acetone in the dark at 0 °C for 24 h. Canthaxanthin (50 μL in acetone) was added as an internal standard in all samples. Prior to analysis, the pigment extracts were vortexed and centrifuged to remove cellular debris.

Subsamples were injected into a Varian 9012 HPLC system equipped with Varian 9300 autosampler, a Timberline column heater (26 °C), and Spherisorb 5 μm ODS2 analytical column (4.6 × 250 mm) and corresponding guard cartridge. Eluting peaks were monitored with a UV/vis absorption diode array detector (436 and 450 nm). Pigment identifications were based on absorbance spectra, co-chromatography with standards and relative retention time.

2.3. Community composition and biomass

FCM and microscopical assessments of microbial community abundance and biomass were made as described by Brown et al. (2008). FCM analyses distinguished population abundances of heterotrophic bacteria, photosynthetic bacteria (*Prochlorococcus* and *Synechococcus* spp.) and photosynthetic eukaryotes. Epifluorescence and inverted microscopy techniques were used to assess abundances, sizes and biovolumes of auto- and heterotrophic protists.

FCM samples (1 mL) were preserved with paraformaldehyde (0.5% final concentration), flash frozen in liquid nitrogen and later transferred to storage in a −85 °C freezer until analysis. Samples were thawed and stained with Hoechst 34442 (1 μg mL^{-1}, final concentration) for one hour at room temperature in the dark (Monger and Landry, 1993; Campbell and Vaulot, 1993). Internal standards of auto-fluorescent polystyrene beads were added to normalize scatter and fluorescence signals. Populations were analyzed with a Beckman–Coulter Altra flow cytometer equipped with two argon ion lasers (1 W of 488 nm and 200 mW of UV excitation). Scatter (side and forward), and fluorescence signals

were collected using filters as appropriate, including those for Hoechst-bound DNA, phycoerythrin and chlorophyll. Populations were distinguished based on distinctive scatter and fluorescence signals from listmode files (FCS 2.0 format, Expo32; Beckman–Coulter) using FlowJo software (Tree Star, Inc., www.flowjo.com). Carbon biomass estimates were computed from FCM measured abundances using factors of 100 fg C cell^{-1} for *Synechococcus* and 32 fg C cell^{-1} for *Prochlorococcus* in the upper euphotic zone (Landry and Kirchman, 2002), with up to a 2-fold increase in the lower euphotic zone in proportion to increasing side scatter.

Protists, including diatoms and other eukaryotic phytoplankton as well as non-pigmented single-cell heterotrophs (grazers), were enumerated microscopically by methods optimized for different size classes and groups. Cells $<10\,\mu m$ were analyzed by epifluorescence microscopy (EPI at 400 ×) on slides prepared with paraformaldehyde-preserved samples (50 mL; 0.5% final concentration) filtered onto 0.8-μm black polycarbonate filters (Brown et al., 2003). Cells $>10\,\mu m$ also were analyzed by EPI (250 ×) on 250-mL samples preserved according to Sherr and Sherr (1993) and filtered onto 8.0-μm polycarbonate filters. Both preparations were stained with proflavin (0.33%) and the DNA-specific fluorochrome DAPI (50 mg mL^{-1}). EPI slides were imaged and digitized on shipboard with an inverted Olympus IX71 microscope and MacroFire color camera. Counting and sizing was automated with ImagePro software, and length and width measurements were converted to biovolumes by applying appropriate geometric shapes. Cellular carbon estimates were calculated from biovolumes according to Eppley et al. (1970).

Diatoms, ciliates and other >20-μm protists also were enumerated and sized by bright-field inverted microscopy on settled, acid Lugol's preserved (1% final concentration) samples (Yang et al., 2004). For these analyses, biovolume-carbon conversions for diatoms and dinoflagellates were based on Menden-Deuer and Lessard (2000). Ciliate carbon estimates were based on Verity and Langdon (1984) and Putt and Stoecker (1989) for loricate and naked forms, respectively.

2.4. Growth, grazing and production estimates

Instantaneous rates of phytoplankton growth (μ) and mortality losses (m) to microzooplankton grazing were estimated from dilution incubations according to Landry et al. (1984). For the undiluted seawater treatment, the net rate of change (k) of any given measured parameter (pigment or FCM population) is $k = \mu - m$. Assuming similar growth rate (μ) in the diluted treatment, the net rate of change $k_d = \mu - x*m$, where "x" = the fraction of natural grazer density in the dilute treatment (0.37 in these experiments). From measured differences in the net rates of population change in the two treatments, the two equations were solved for the two unknowns, μ and m.

$$m = (k_d - k)/(1 - x) \quad \text{and} \quad \mu = k + m$$

Net growth rate estimates k exceeded k_d on a few occasions in these analyses, typically toward the base of the euphotic zone where the net rates and the population concentrations were both low and difficult to measure. For these results, μ was set as the measured rate of change in the undiluted bottle, which was assumed to represent a minimal reliable estimate of μ since it involved no experimental manipulation and had a higher measurement signal than the dilute bottle. Using this alternative means of determining μ introduced a very slight positive bias in the mean estimates of growth rates (e.g., 0.009 d^{-1} for total chlorophyll *a*). The lack of nutrient-added treatments in the experimental design may also mean that the computed rates could be underestimates. We, however, did not observe a systematic bias in comparing the results from 2-bottle *in situ* experiments to several full dilution experiments with nutrient treatments (e.g., Landry et al., 1998) that were done on shipboard.

Experimental estimates of μ and m were used to compute community and taxon-specific biomass rates of phytoplankton production and grazing according to Landry et al. (2000b). Production estimates (mg C m^{-3} d^{-1}) were calculated as

$$PP = \mu * C_0(e^{(\mu - m)t} - 1)/(\mu - m)t$$

where C_0 is initial biomass in mg C m^{-3} and $t = 1$ day. Similarly, the biomass consumption of microzooplankton was computed as

$$PG = m * C_0(e^{(\mu - m)t} - 1)/(\mu - m)t$$

From this, we estimated the biomass-specific ingestion rate of microzooplankton feeding on phytoplankton (i.e., % body C consumed d^{-1}) as $PG*100/B_H$, where B_H is the estimated carbon biomass of heterotrophic protists (mg C m^{-3}). Lastly, we determined the biomass-specific clearance rate of heterotrophic protists (volume cleared mg C^{-1} d^{-1}) as $m*B_H^{-1}$. Statistical tests of rate differences from the experiments were made by the non-parametric Mann–Whitney U test, double-sided (Tate and Clelland, 1957).

3. Results

3.1. Community rate profiles

Community growth and grazing estimates from total chlorophyll *a* (TChl *a*) were quite variable within and between experimental incubations (Fig. 1). Mean coefficients of variability (CV) were lower for OUT station estimates compared to IN stations (e.g., CV = 28% vs 40% for all experiments within depth range averages of Fig. 2), and OUT stations were more coherent in terms of mean estimates and pattern (e.g., μ maxima in the lower euphotic zone). Nonetheless, 4 of 5 IN profiles showed mid-euphotic zone minima in growth rates around 60 m. For both IN and OUT profiles, growth was generally in excess of grazing in the mid-euphotic zone with occasional balances in near-surface and deep incubations (Fig. 1).

Because of the variability in individual profiles, the differences among IN and OUT stations are more fruitfully explored as averages. In Fig. 2, for example, mean characteristics divide the euphotic zone into upper and lower regions. The upper zone includes experiments conducted at 10 and 30–40 m, roughly defining the surface mixed layer. There were slight IN–OUT differences in TChl *a* and phytoplankton biomass in this upper layer, but growth rates were substantially and significantly elevated at the IN stations (0.51 vs 0.31 d^{-1}; $0.01 < p < 0.05$). In contrast, growth rates showed little difference between IN and OUT profiles in the lower layer (50–110 m), whereas phytoplankton carbon and TChl *a* were both strongly elevated in the eddy.

3.2. Taxon-specific growth rates

Euphotic zone differences in growth versus biomass effects for the phytoplankton community (Fig. 2) also extend to many of the component populations. The photosynthetic bacterium *Prochlorococcus* (PRO), for instance, showed an inconsistent biomass response in the upper 40 m, with cell abundance slightly lower and divinyl chlorophyll *a* (DVChl *a*, a diagnostic pigment of PRO) slightly higher at IN versus OUT stations (Fig. 3). These differences suggest an increase in cellular chlorophyll content at the IN stations, one potential indicator of enhanced physiological state. As a further indication of physiological enhancement, growth rates (μ) were clearly elevated within this upper zone in the eddy

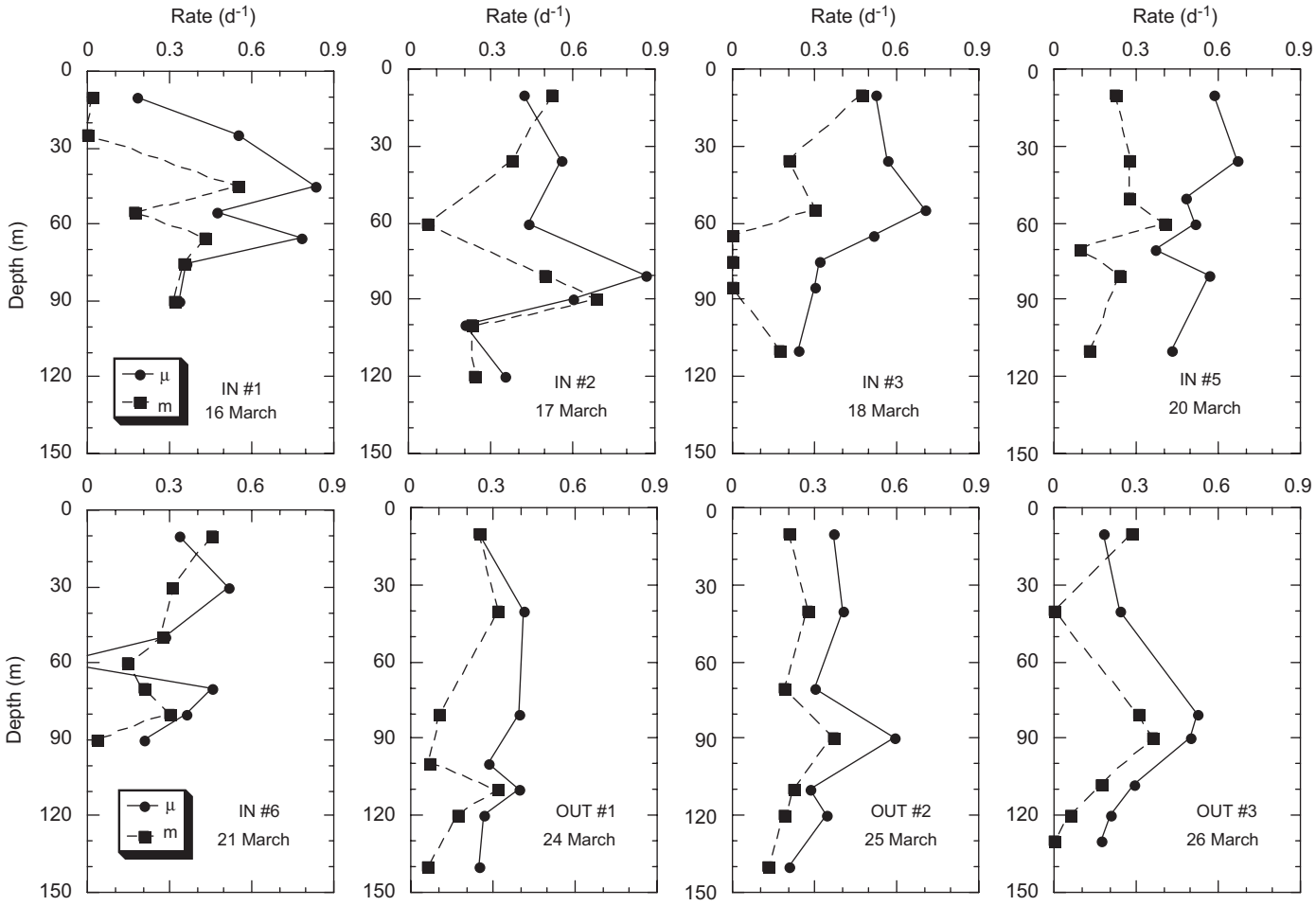

Fig. 1. Depth profiles of phytoplankton growth (μ) and microzooplankton grazing (*m*) for *in situ* dilution incubations in the central region of Cyclone *Opal* (IN) and at control stations (OUT). Experiment numbers and dates as indicated; no experiments were conducted on IN day #4. Rate estimates are based on measured changes in TChl *a*.

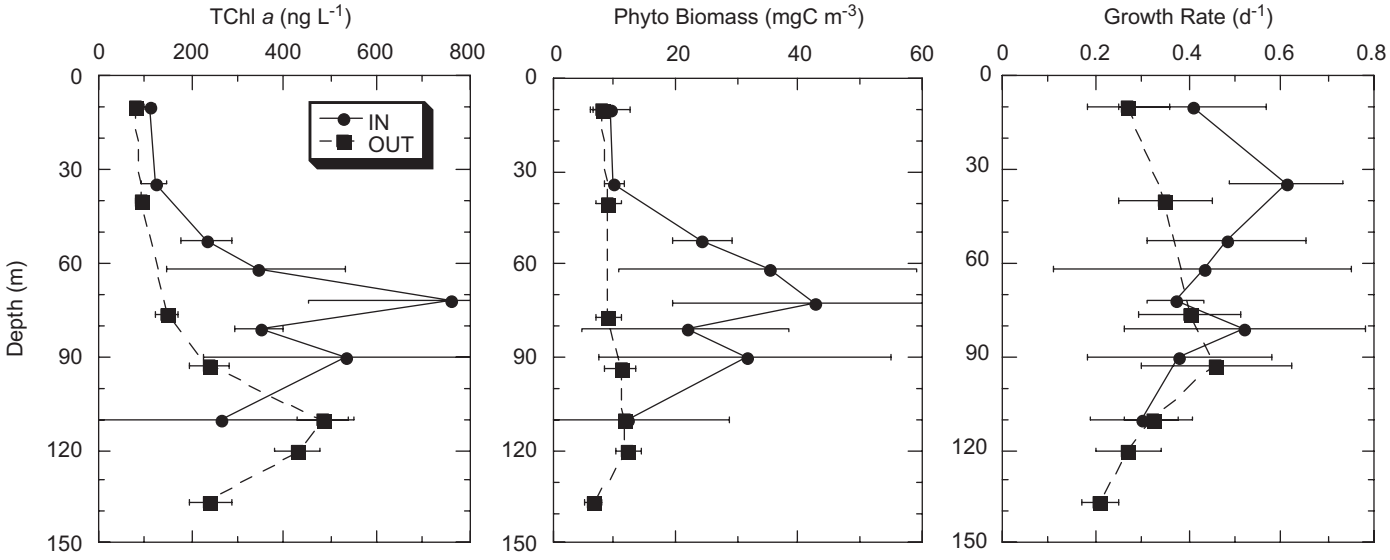

Fig. 2. Mean depth profiles for TChl *a*, phytoplankton carbon biomass and phytoplankton community growth rates from *in situ* dilution incubations conducted IN and OUT of Cyclone *Opal*. Growth rate estimates are based on TChl *a*. Error bars are standard deviations.

relative to control stations as estimated either by DVChl *a* (0.64 vs $0.38\,d^{-1}$; $p = 0.01$) or by cell abundance (0.68 vs $0.45\,d^{-1}$; $p = 0.05$). Both cell abundance and growth rates dropped precipitously below 60 m for PRO at the IN stations, whereas OUT stations showed maxima in DVChl *a*, cells and μ in the depth range of 90–110 m (Fig. 3). Peaks in DVChl *a*, PRO cells and growth rate were shifted upwards by 50–60 m in Cyclone *Opal* relative to OUT profiles. Abundance and pigment peaks were lower in the

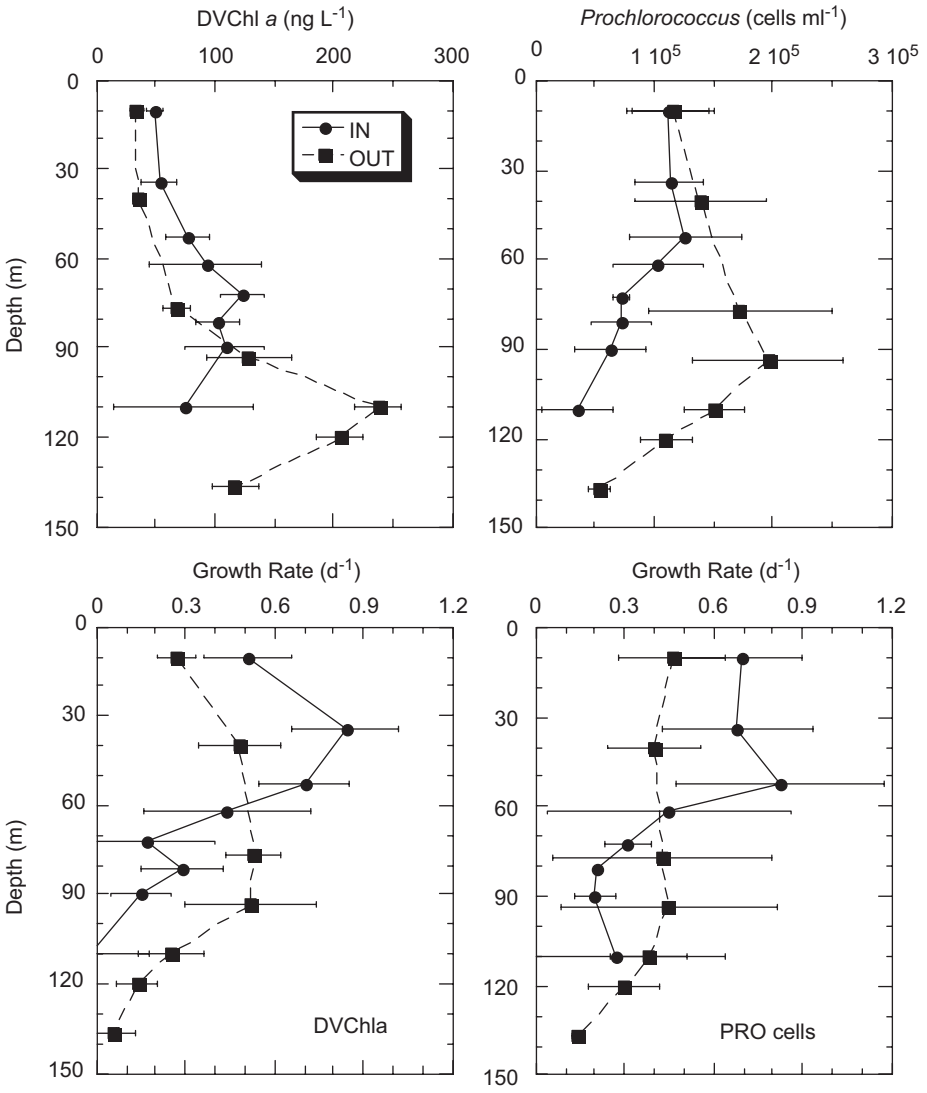

Fig. 3. Mean depth profiles for divinyl chlorophyll *a* (DVChl *a*), *Prochlorococcus* spp. cell density and PRO growth rates from *in situ* dilution incubations conducted IN and OUT of Cyclone *Opal*. Growth rate estimates are based on DVChl *a* (left) and on cell counts from flow cytometry (right). Error bars are standard deviations.

eddy, as were depth-integrated totals for the euphotic zone compared to OUT stations.

Complementary analyses by HPLC and FCM methods in Fig. 3 provide a rare opportunity to directly compare PRO growth rates estimates from DVChl *a* and cell abundance in a significant set of dilution experiments spanning the entire euphotic zone and incubated under *in situ* conditions. The profile patterns differ somewhat in detail, but show overall good agreement in terms of mean rates and the salient differences between IN and OUT stations. In further analyses of production patterns below, we use μ estimates from DVChl *a* as the more reliable measure of PRO growth rate because they are based on samples of a more robust size (2 L vs 100 μL) and therefore exhibit less variability. The pigment-based analyses also minimize complications in distinguishing very dim cells by FCM in the upper layer.

Compared to PRO, diatoms were strongly enhanced as pigment and biomass in the mid- to lower euphotic zone of Cycle *Opal* relative to their negligible background concentrations at control sites (Fig. 4). No clear pattern emerged for IN–OUT differences in mean diatom growth rate. We note, however, that the diatom growth rate profile for IN stations shows a mid-depth minimum ($0.20\,d^{-1}$) at 50–65 m, which is significantly different from mean growth rates in shallower ($0.54\,d^{-1}$, 10–45 m; $p<0.01$) and deeper ($0.53\,d^{-1}$, 70–90 m; $p<0.01$) waters. This zone of apparent low diatom growth corresponds to the upper shoulder of the diatom biomass increase with depth. In contrast, the depth range of peak diatom carbon and pigments at 70–90 m is a zone of relatively high growth rate.

Taken together, the biomass of all "other" phytoplankton (i.e., after PRO and diatom carbon contributions were subtracted from the total) was not markedly different between IN and OUT stations, with the IN profile looking like little more than a 50-m shoaling of the OUT profile (Fig. 5). Among the taxa that comprise these "other" phytoplankton, prymnesiophytes and pelagophytes (as indicated by diagnostic pigments 19′-HEXanoyloxyfucoxanthin and 19′-BUTanoyloxyfucoxanthin, respectively) showed growth rate enhancement in the upper euphotic zone, extending into the diatom maximum zone for BUT (upper panels, Fig. 5). Growth rates based on FCM analyses of picoeukaryotes (PEUKs) were consistent with these pigment inferences, both in terms of general magnitude and upper-layer enhancement. However, the PEUK estimates were noisy because their numbers were relatively

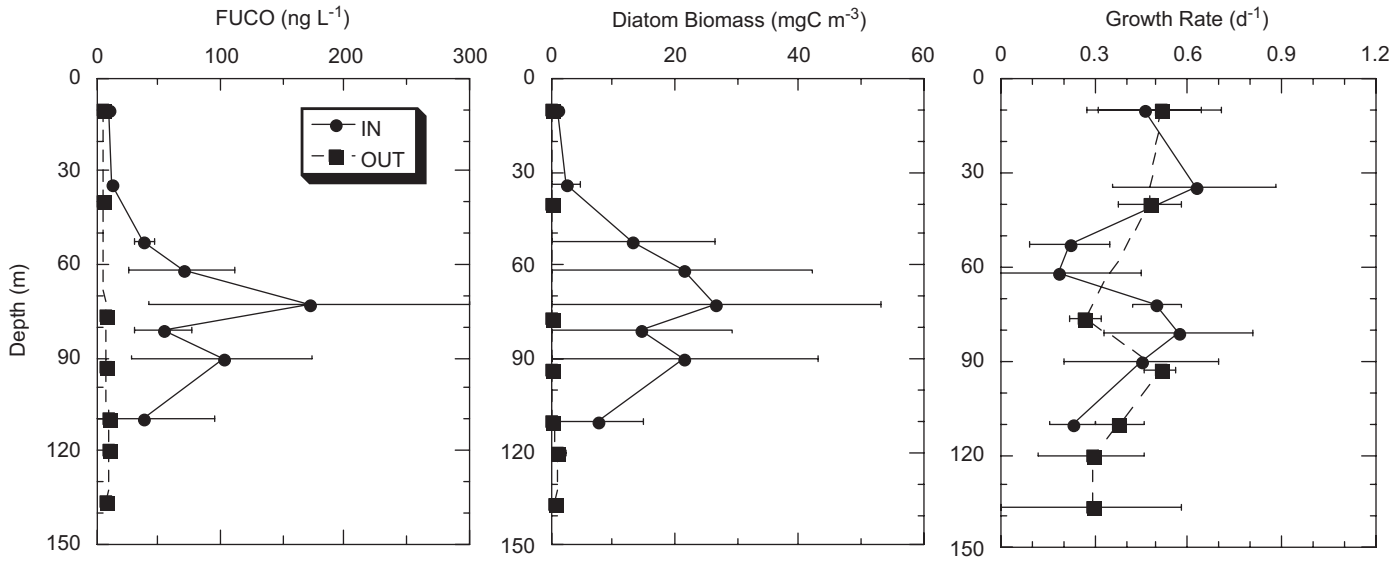

Fig. 4. Mean depth profiles for fucoxanthin (FUCO), diatom carbon biomass and growth rate estimates for diatoms from *in situ* dilution incubations conducted IN and OUT of Cyclone *Opal*. Growth rate estimates are based on FUCO. Error bars are standard deviations.

low and the volumes analyzed (100 μL) small. The same also can be said for SYN rate estimates from flow cytometry. This does not explain, however, the curious result of decreased SYN growth rate in the upper layer of Cyclone *Opal* versus estimated rates at the OUT stations.

3.3. Phytoplankton production

Production estimates from the dilution experiments are essentially the product of growth and biomass measurements, and therefore combine these two effects when comparing IN and OUT experimental results. Thus, it is not surprising that production estimates were enhanced throughout the euphotic zone of Cyclone *Opal*, and particularly so in the deep layer of high diatom biomass and growth rate (Fig. 6). Maximum rates in the 60–70 m depth range are 20–30 mg C m^{-3} d^{-1}, exceeding production estimates at OUT stations by 4–6 fold. PRO contributed about 50% of total production in the upper euphotic zone for both IN and OUT stations. However, this contribution dropped sharply in the eddy below the mixed layer, whereas it continued to increase in importance with depth in the OUT stations, accounting for 65–70% of total phytoplankton production in the 70–90 m depth range.

Diatom contribution to phytoplankton production was enhanced throughout the eddy euphotic zone, but maximal effects, exceeding 80% of production, were clearly in the 70–90-m depth horizon (Fig. 6). The diatom dominance of this zone in the eddy provides a particularly sharp contrast to PRO dominance of the depth range in ambient waters. The two groups essentially switched their dominance and background roles in the nutrient-perturbed portion of the eddy's euphotic zone.

Viewing the IN station production results as a time-series underlines the point that the eddy-induced diatom bloom was in a state of decline throughout most of the period of observation (Fig. 7). Initial depth-integrated production in Cyclone *Opal* was about 3 times higher than OUT-station estimates. Over the course of six days, however, eddy production fell to ambient values, although the contributions of diatoms and PRO had not yet adjusted to the mean characteristics of OUT stations. Peak estimates of integrated diatom production were 44-times higher than mean ambient values, and the highest diatom production in the region of high biomass exceeded mean background levels by more than a factor of 200.

3.4. Grazing relationships

Grazing rate estimates for total phytoplankton, PRO and diatoms (from TChl *a*, DVChl *a* and fucoxanthin (FUCO) pigments, respectively) largely reflected production rate patterns, with consumption of PRO strongest in the upper euphotic zone of Cyclone *Opal* and diatom consumption dominant in the lower euphotic zone (Fig. 8, upper panels). On a depth-integrated basis, microzooplankton consumed 55% of total phytoplankton production in the eddy and 60% at OUT stations (Fig. 8, lower left). On average, depth-integrated estimates were slightly higher for PRO, and similar between IN and OUT profiles (65% vs 63%, respectively; Fig. 8, lower middle). The percentage of diatom production grazed was also similar for the upper 60 m of IN and OUT profiles but diverged sharply below, with OUT stations showing higher % grazing of deep living diatoms and the IN profiles, indicating markedly depressed grazing (mean ~40% of diatom production) in the depth range of high concentration (Fig. 8, bottom right). Overall, 58% of depth-integrated diatom production was grazed IN Cyclone *Opal* and 75% at OUT stations.

As also noted by Brown et al. (2008), the biomass of microzooplankton grazers was enhanced in Cyclone *Opal*, and the increase was more or less uniformly distributed over the euphotic zone (Fig. 9). In the upper mixed layer, grazing impact increased in proportion to increased grazer biomass such that biomass-specific ingestion and clearance rates were virtually identical between IN and OUT stations. This was not the case, however, in the diatom-rich lower euphotic zone, where biomass-specific consumption rates approximately tripled (from ~50% to 150% body C d^{-1}) even as clearance efficiency decreased relative to OUT stations (Fig. 9).

4. Discussion

Cyclone *Opal* was a significant eddy in terms of its size (200–220 km diameter) and perturbation of the water-column

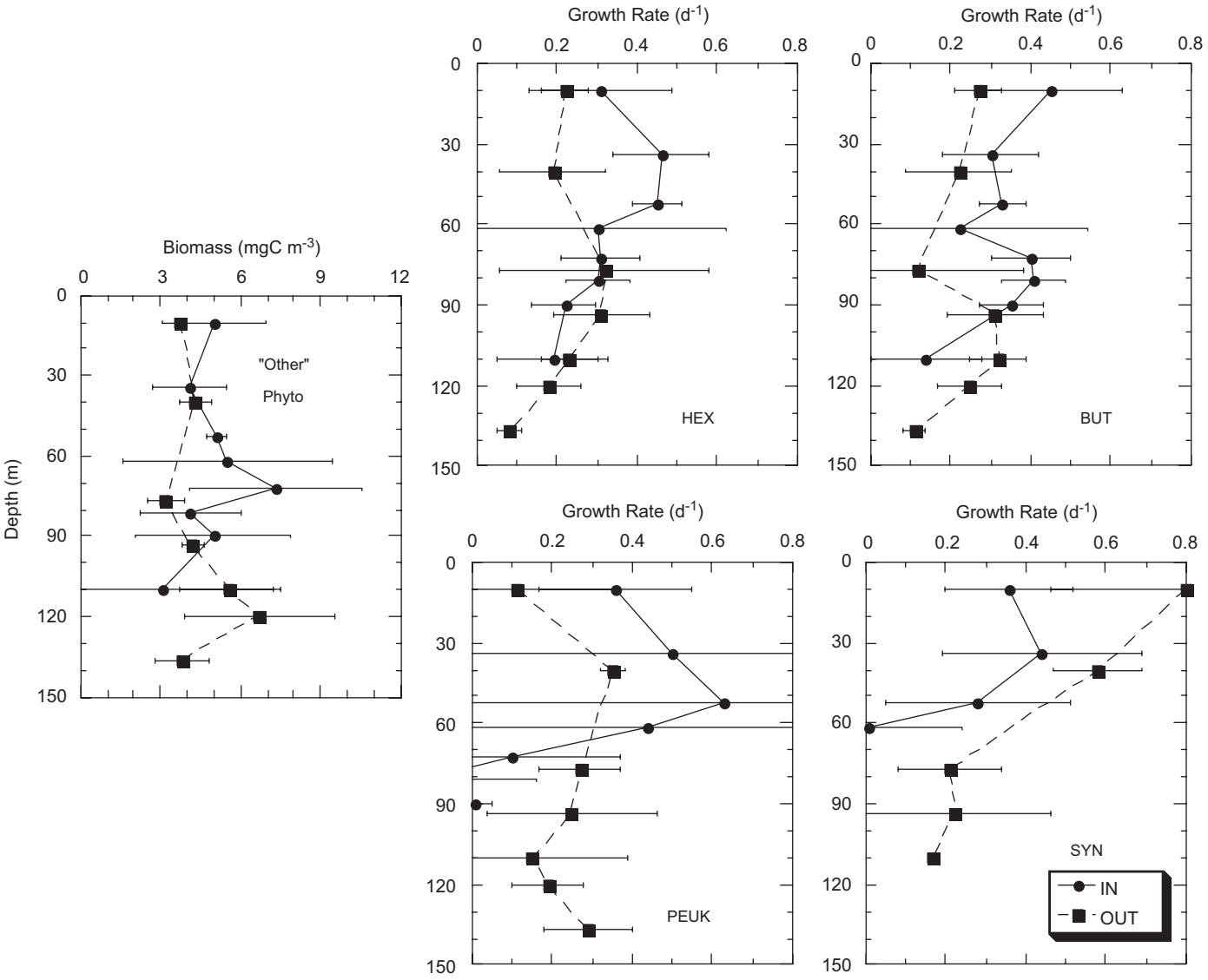

Fig. 5. Mean depth profiles for carbon biomass of "other phytoplankton" (i.e., phytoplankton other than *Prochlorococcus* or diatoms) and growth rate estimates for selected populations. Growth rate estimates are based on measured change in the pigments 19′-hexanoyloxyfucoxanthin (HEX) and 19′-butanoyloxyfucoxanthin (BUT) and flow cytometric estimates of pico-eukaryotic algae (PEUK) and *Synechococcus* (SYN). Profiles are truncated at depths where concentrations were too low for numerical analyses. Error bars are standard deviations.

density structure. The sigma–*t* density surface of 24 kg m^{-3} occurred at ~50 m depth on average, and as shallow as 42 m, in the eddy core, uplifted from depths of ~130–150 m in surrounding waters. As expected for a nutricline displacement of this magnitude, plankton biomass, productivity and community composition in the mid- to lower euphotic zone of Cyclone *Opal* were profoundly impacted by the massive input of new nutrients. However, only subtle nutrient enrichment effects extended into the mixed layer, creating highly contrasting systems in the upper and lower euphotic zones.

Cyclone *Opal* is, to our knowledge, the first oceanic mesoscale eddy whose microplankton community has been studied with experimental techniques designed to reveal the depth variability of process rates and taxon-specific contributions to community dynamics and production. In the discussion below, we highlight the contrasting dynamics of *Prochlorococcus* and diatoms in the eddy depth profiles. *Prochlorococcus* (PRO) is the archetypical primary producer in the oligotrophic open ocean. Large chain-forming diatoms typically dominate nutrient-enriched conditions in turbulent shallow mixed layers. Although these very different phytoplankters occupy extreme ends of the ecological spectrum for ocean variability, each was significantly enhanced by the eddy but dominated a different region of the stratified water column.

4.1. Experimental constraints, tradeoffs and interpretations

Because the light and temperature regimes experienced by phytoplankton in the lower euphotic zone are difficult to reproduce in shipboard incubators, it was critical to the comparison of process rates to conduct our experiments under *in situ* conditions. We therefore, adapted a compact version of the dilution technique (Landry et al., 1984) for this study, using only two unreplicated treatments per depth.

In previous experience with this technique in the central equatorial Pacific (December 2004), we evaluated its experimental

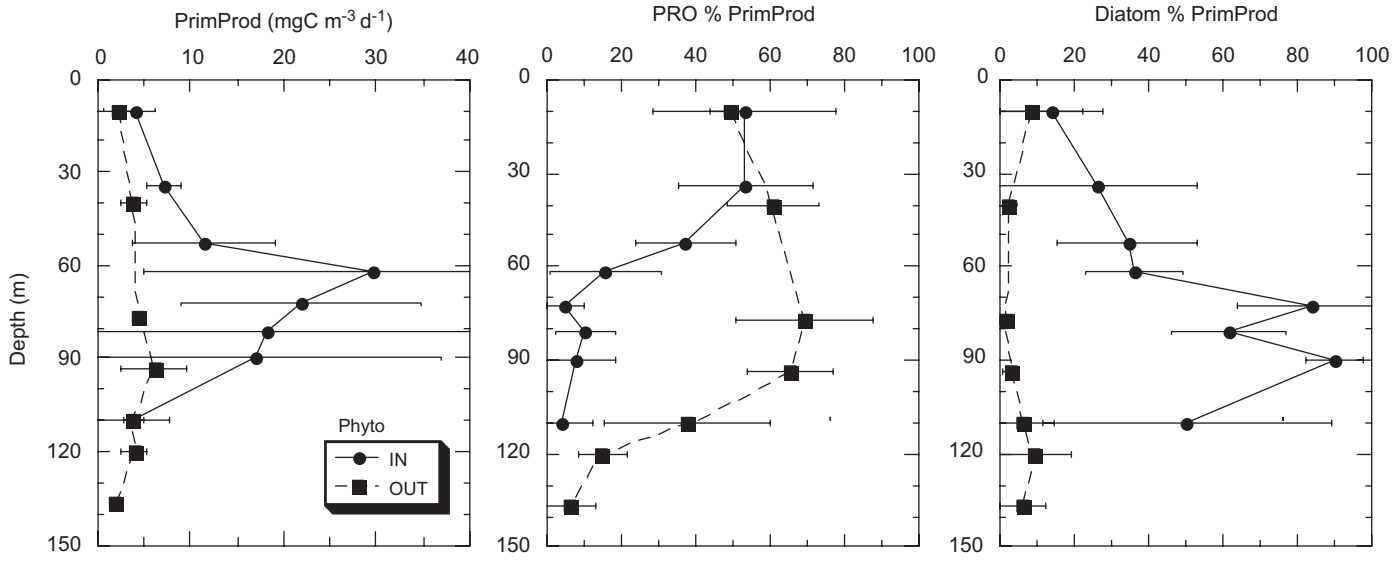

Fig. 6. Mean depth profiles for total community estimates of primary production (PrimProd) and percentages ascribed to *Prochlorococcus* (PRO) and diatoms from *in situ* dilution incubations conducted IN and OUT of Cyclone *Opal*. Error bars are standard deviations.

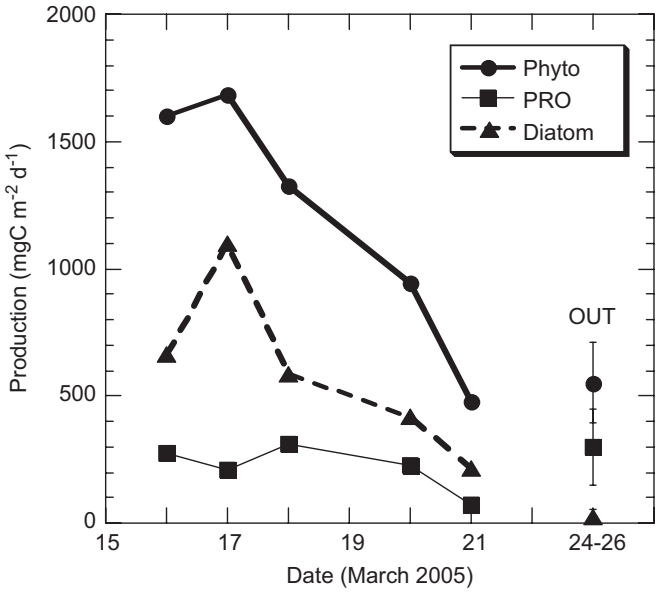

Fig. 7. Depth-integrated estimates of total phytoplankton primary production (Phyto) and production attributed to *Prochlorococcus* (PRO) and diatoms from *in situ* dilution incubations conducted IN and OUT of Cyclone *Opal*. Daily estimates are for individual experimental dates at IN stations, as given in Fig. 1. Three OUT station estimates are averaged for March 24–26; error bars are standard deviations.

variability from the results of triplicate experiments run on 19 occasions, where each experiment was prepared from water collected and processed independently from separate water bottles (i.e. not pseudoreplicates). This large data set gave mean standard deviations of 0.07 and 0.10 d^{-1}, respectively, for growth (μ) and grazing (m) estimates from the upper mixed layer (Landry et al., 2005). The experiments also, however, gave extraordinarily reproducible depth profiles of rate estimates from stations separated days to weeks and 100s to 1000s of km apart. It is therefore not clear whether the low variability in equatorial waters can be ascribed to methodological precision or to the uniformity and chemostat qualities of that ocean-upwelling region. In comparison, the magnitude of variability in the Cyclone *Opal* rate profiles (e.g., Fig. 1) was much more pronounced. Given the highly stratified structure of the eddy core region and its evolving characteristics during the study period, at least part of the variability must reflect real day-to-day differences in the initial physiological states and environmental circumstances at the depths and locations where the water samples were taken. There is, however, no clear-cut approach for distinguishing the contributions of different factors to the variability observed.

In the absence of designed replication, interpretations of the resulting data set were aided by averaging depth profiles for experiments conducted on different days. This procedure is conservative in smearing effects that evolved with time or depth and in de-emphasizes the extreme contrasts that might be made between IN and OUT stations. Nonetheless, it has the advantage of focusing attention on statistically significant and spatially robust effects that persisted over several days of study.

4.2. Phytoplankton dynamics in the upper mixed layer (0–40 m)

Although the spatial gradients in Cyclone *Opal* were complex and changing over the course of our study, we can, for the sake of discussion, view the euphotic zone in the core region as divided into three depth strata—the upper mixed layer, the deep euphotic zone, and an intermediate layer of diatom senescence.

The upper mixed layer of Cyclone *Opal* averaged ~40-m deep and largely retained the community compositional characteristics of surrounding waters throughout the period of study (Brown et al., 2008). Mean mixed-layer TChl *a* concentration was slightly higher in the eddy center than in ambient waters (Fig. 2), and there were measurable, though modest, indications of eddy entrainment of cooler and more saline water (Dickey et al., 2008).

Despite the lack of a strong biomass response, physiological indices and rate estimates suggest that mixing or diffusion provided some nutrient enhancement to the mixed layer. For example, variable fluorescence (F_v/F_m) was stimulated at the base of the mixed layer (40 m) in the eddy core (Bibby et al., 2008), indicating a general physiological shift-up of the resident phytoplankton assemblage there. The ratio of DVChl *a* to PRO cells was elevated in the surface mixed layer of the eddy (Fig. 3), and FCM analyses of PRO cells indicated a modest, though

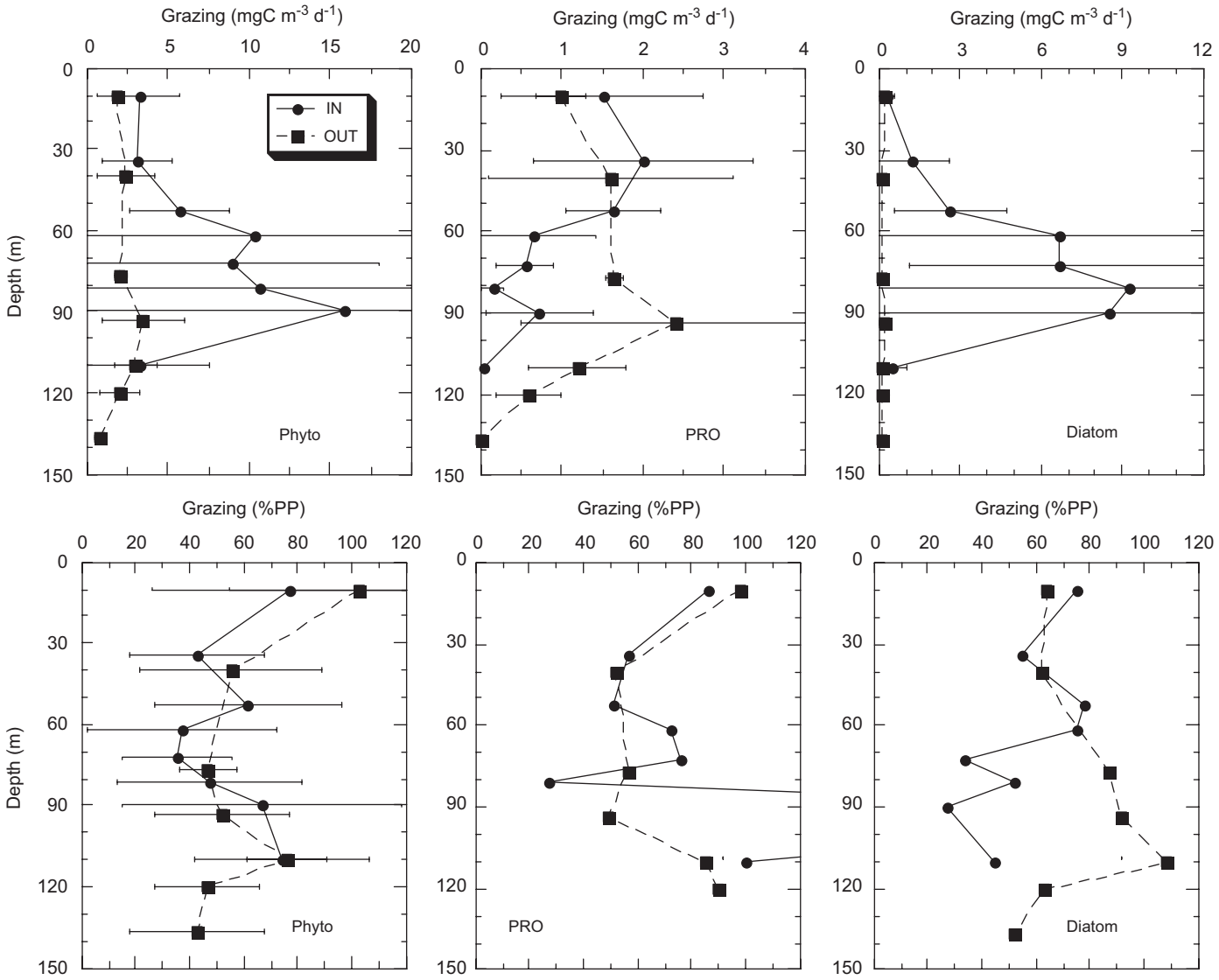

Fig. 8. Mean depth profiles for grazing estimates on total phytoplankton primary production (Phyto) and production attributed to *Prochlorococcus* (PRO) and diatoms. Upper panels are for microzooplankton grazing rates expressed as biomass consumed ($mg\,C\,m^{-3}\,d^{-1}$). Lower panels are for estimates expressed as percent of production of the total community (Phyto) and as percent of the production attributed specifically to PRO or diatoms. Error bars are standard deviations.

significant, 9% increase in cellular red fluorescence, a measure of chlorophyll content, in *Opal* mixed-layer samples compared to OUT stations. Growth rates of PRO and other small phytoplankton, such as prymnesiophytes and pelagophytes, were significantly elevated above ambient levels in the eddy mixed layer (Figs. 3 and 5), and grazing rates increased in proportion to the elevated biomass of microzooplankton (Fig. 9). These effects are similar in many respects to observations of enhanced physiology and turnover rates of pico- and nano-phytoplankton in open-ocean fertilization experiments. In IronEx II, for example, there was little evidence of an iron fertilization effect on biomass or composition of cells less than 10 μm (Landry et al., 2000a), but their growth rates and physiological states were clearly stimulated (Cavender-Bares et al., 1999; Landry et al., 2000b; Mann and Chisholm, 2000).

Diatom biomass increased in the mixed layer of Cyclone *Opal* by about $1\,\mu g\,C\,L^{-1}$, which significantly ($p<0.01$) increased the contribution of diatoms to total community production in this layer (Fig. 6). In other respects, however, the *Opal* mixed layer was remarkable in terms of its stimulation of the entire phytoplankton community such that the dominance and relative contribution of PRO to total community production (~50%) remained virtually unchanged (Fig. 6). In effect, nutrients infused into the surface layer of Cyclone *Opal* appear to have been locked into the cycle of rapid turnover and recycling characteristic of oligotrophic waters like the subtropical North Pacific.

4.3. The intermediate zone (50–60 m)

Deep isopycnals (sigma–$t = 24\,kg\,m^{-3}$) from 130 to 150 m in surrounding waters were uplifted to 50–60 m in Cyclone *Opal*, between the base of the mixed layer and the deeper diatom maximum. Being a depth zone of greater light intensity (5–10% of surface) than the waters below, it is the logical place for a diatom bloom to have started in response to the input of new nutrients. The residual assemblage of senescent diatoms provides evidence of that early history. We also can reasonably surmise that diel or day-to-day variability in the depth of the overlying mixed layer would have eroded the boundary between these strata to bring some nutrients and diatoms into the upper waters (along with the modest temperature and salinity signals observed). The dynamics

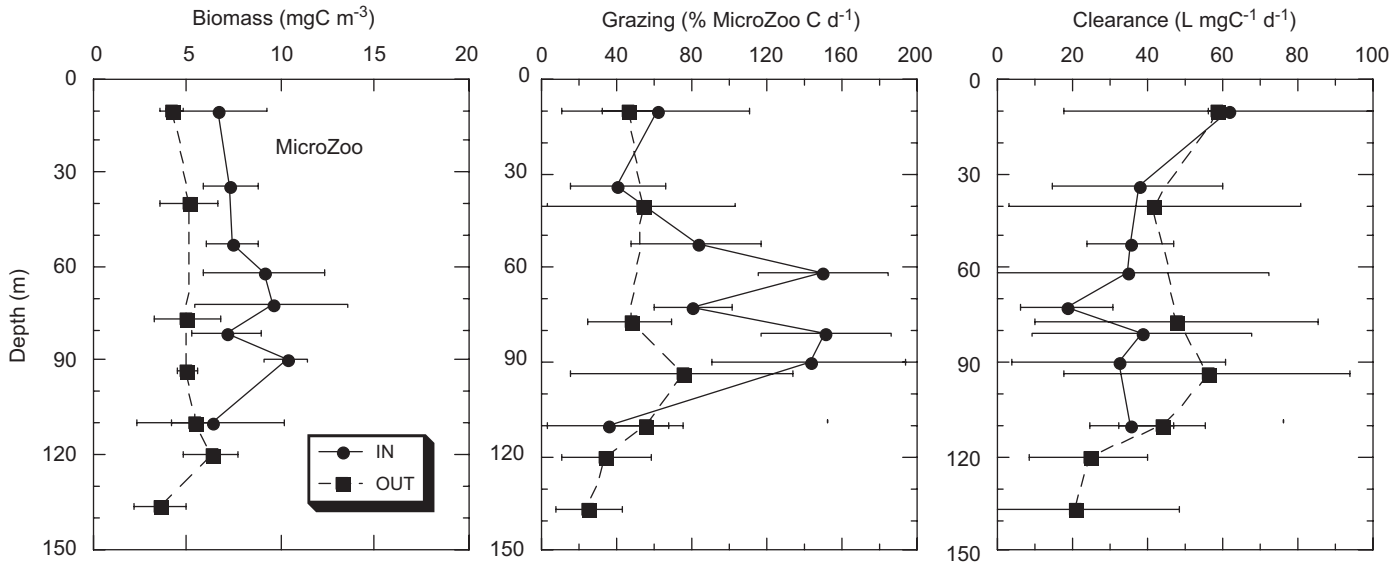

Fig. 9. Mean depth profiles for microzooplankton biomass and grazing rates from *in situ* dilution incubations conducted IN and OUT of Cyclone *Opal*. Grazing estimates are presented as percent of microzooplankton carbon consumed (% MicroZoo C d^{-1}) and as biomass-specific clearance rates (L mg C^{-1} d^{-1}). Error bars are standard deviations.

of this zone are therefore linked to those of both the upper and lower euphotic zones.

In the present study, the 50–60 m depth range was defined by strong gradients. Concentrations of pigments and phytoplankton biomass increased with depth through this region, while growth rate estimates generally declined (Figs. 2–5). These gradients mark a strong transition from *Prochlorococcus* dominance of primary production in surface waters and diatom dominance of the deep euphotic zone (Fig. 6). PRO cell abundance was not notably depressed in this transition zone relative to the mixed layer, but growth rates dropped sharply with depth (Fig. 3). However, while PRO growth rates declined more-or-less monotonically through the deep euphotic zone, the intermediate zone represented only a local minimum in diatom growth.

Low growth rates of diatoms in the 50–60 m depth range are consistent with the observations of senescent diatoms and empty frustules in this layer (Brown et al., 2008). Benitez-Nelson et al. (2007) and Rii et al. (2008) have suggested that the unhealthy state of diatoms in this stratum was likely due to very low concentrations of dissolved silicate (i.e., Si limitation). Nencioli et al. (2008) have further proposed that 70 m is approximately the lower depth at which the core region of Cyclone *Opal* behaved as a "closed" system, cut off from nutrient replenishment from radial flows along isopycnal surfaces as the eddy moved from north to south. Microzooplankton grazing was not significantly elevated in this stratum, but given the depressed growth rates of diatoms, it is the only portion of the euphotic zone where microzooplankton grazing on diatoms was in balance with diatom growth (mean μ and $m = 0.23$ and 0.21 d^{-1}, respectively). Thus, additional losses of cells to sinking or mesozooplankton grazing would make it a zone of net diatom decline.

4.4. The lower euphotic zone (70–90 m)

In marked contrast to the upper mixed layer, the lower euphotic zone of *Opal* exhibited a strong signal in biomass accumulation, dominated by large centric diatoms, especially *Chaetoceros* and *Rhizosolenia* spp. (Brown et al., 2008). Diatom biomass was maximum at about 70 m, but growth rates were substantial, averaging 0.51 d^{-1}, throughout the depth range of 70–90 m. In their "open-bottom, horizontally leaky" hypothesis for Cyclone *Opal* physical flows, Nencioli et al. (2008) highlight the 70–90 m depth strata as the place where horizontal water exchange, and nutrient refreshment (from ~150 m in surrounding waters), could occur along density surfaces (sigma–t = 23.6–24.2 kg m^{-3}) as the eddy moved. The faster growth and better physiological condition observed for diatom cells in this depth range may therefore reflect special physical circumstances in this stratum rather than the transient state of a bloom that is gradually working its way deeper in the euphotic zone. Nonetheless, since light intensities were relatively low from 70 to 90 m (typically 1–5% of incident PAR), measured growth rates were likely well below physiological potential, reflecting the tradeoffs between declining light and increasing nutrients with depth. In comparison, Landry et al. (1998) found a growth rate of 2.7 d^{-1} for a surface bloom of *Chaetoceros curvisetus* during SW Monsoon upwelling in the Arabian Sea.

In order to accumulate the deep maximum of diatom biomass observed in Cyclone *Opal*, ~100 times background levels, diatom growth rates must have exceeded loss processes for a significant period of time prior to our arrival. This likely occurred as sharp decoupling of growth and grazing during the initial response of large diatoms to the doming of nutrient-rich isopycnals into the euphotic zone. Population seeding of the deeper (70–90 m) layer, and perhaps the sinking of significant biomass, also may have occurred as nutrients became depleted in overlying waters. Even during our relatively late period of observation when diatom biomass was declining, microzooplankton grazing rates on diatoms were lowest as a percentage of growth and production in the deep layer of high diatom biomass than elsewhere in the euphotic zone (Fig. 8). Similarly, the apparent efficiency of microzooplankton grazing on phytoplankton, estimated as biomass-specific clearance rate, was depressed throughout the depth range dominated by diatoms compared to control sites (Fig. 9).

Cyclone *Opal* was unique among previously observed eddies in the lee of the Hawaiian Islands in producing a dramatic response of large diatoms, as opposed to dinoflagellates or prymnesiophytes (e.g., Bidigare et al., 2003; Vaillancourt et al., 2003). As suggested by Rii et al. (2008), this may have more to do with conditions (e.g., a large, rapid nutrient perturbation) that select for large diatoms over the small phytoplankton that more

typically characterize the oligotrophic open ocean. The phytoplankton dynamics of Hawaiian lee cyclones may therefore be set by spin-up conditions rather than following a fixed pattern of succession defined by eddy age (Sweeney et al., 2003). The present results are relevant to this discussion because they show two very distinct community responses existing at the same time in the same eddy separated by only 30 m of water column.

4.5. Microzooplankton grazing and the fate of diatom production

Microzooplankton consumed 55% of total phytoplankton production in Cyclone *Opal* and 59% at control (OUT) stations. Both estimates are low compared to the global average of grazing impact from dilution experiments (67% of PP), and the mean for open-ocean tropical systems (75% of PP; Calbet and Landry, 2004). It is significant, however, that grazing pressure was similar in magnitude for large diatoms (58% of PP) as for the whole phytoplankton community and not very different, as a proportion of PP consumed, between IN and OUT stations. The relative role of microzooplankton in the trophic ecology in Cyclone *Opal* was therefore surprisingly similar to adjacent subtropical waters. Diatom growth was, however, more decoupled from grazing in the deeper euphotic zone of *Opal*, with microzooplankton consuming only ~40% of production at depths $\geqslant$70 m (Fig. 8). The higher water-column average included the substantial biomass of slower-growing diatoms at 50–60 m (Fig. 4), where mean growth and grazing rates were in reasonable balance (0.23 versus 0.21 d^{-1}).

Large (>50 μm) ciliates and dinoflagellates, the most likely protistan grazers of diatoms, were ~3-times higher than ambient biomass levels in the diatom-enriched regions of Cyclone *Opal* (Brown et al., 2008). Such consumers capture and process their food as individual prey items and produce individual empty frustules as a by-product of grazing (Jacobson and Anderson, 1993; Jeong et al., 2004). Their particulate egesta have therefore quite different implications for organic export of diatom production compared to alternative loss processes, such as the large organically dense fecal pellets of metazooplankton grazers or the mass settling of intact cells as aggregates (e.g., Sarthou et al., 2005). The comparable grazing impacts of microzooplankton in *Opal* and ambient waters suggest that, even in its perturbed state, the eddy remained a system in which tight trophic coupling and efficient recycling may have suppressed export. As noted by Benitez-Nelson et al. (2007), this interpretation is consistent with lack of a strong export signal from the eddy as measured by ^{234}Th and sediment trap methods, with the disproportionate export of biogenic silica as intact empty diatom frustules in sediment traps (Rii et al., 2008), and with the large accumulation of dissolved organic carbon in the deep euphotic zone. Since microzooplankton grazing does not account for all of the production measured in our experiments, or explain the substantial decline in diatom standing stocks that was observed during our study (Fig. 7), we cannot exclude the possibility that more cryptic processes such as viral infection or autolysis (Brussard et al., 1997) may have contributed to the bloom decline and thus also to more efficient recycling within the eddy. However, if such processes dominated, significant net positive growth would not have been observed in our incubation bottles.

High microzooplankton grazing on diatoms is not a unique feature of Cyclone *Opal*. Comparable results (>50% of diatom production or more) have been reported for diatom-favorable conditions such as SW Monsoon upwelling in the Arabian Sea (Brown et al., 2002), the iron-stimulated phytoplankton bloom of IronEx II (Landry et al., 2000a, b) and retreating ice-edge blooms of the Antarctic Polar Front (Landry et al., 2002). Microzooplankton protists as major grazers of diatom production therefore may be more a general characteristic of open-ocean ecosystems than a novel result of this study. The difference in Cyclone *Opal* is the presence of a significant biomass of large diatoms relatively deep in the euphotic zone. Whereas the vacant frustules of small diatoms may typically remain in suspension in well-mixed surface layers and be remineralized and reutilized in place (Bidle and Azam, 1999; Brzezinski et al., 2001), the frustules from *Opal* were sufficiently large and spatially detached from the mixed layer to make their way into sediment traps at 150 m largely devoid of accompanying organic material (Rii et al., 2008). Assuming that dissolved silicate ultimately serves as constraint to diatom production, the selective export of particulate biogenic silica greatly diminishes the amount of organic matter that a system such as *Opal* can export.

5. Conclusion

Experimental studies of microplankton community growth and grazing interactions in Cyclone *Opal* revealed both a rich spatial complexity to the community response and unexpected implications for the coupling of rate processes. Hawaiian wind-generated, first-baroclinic mode eddies such as Cyclone *Opal* can clearly stimulate growth and production of dominant members of the ambient subtropical phytoplankton as well as large exotic diatoms. These results are consistent with the hypothesis that the rates and magnitudes of new nutrient delivery to the euphotic zone have more effect on the resulting community response than the chronological age or phase of an eddy (Rii et al., 2008). Within Cyclone *Opal*, alternative community responses co-existed in time as spatially separated zones of the same water column. Thus, one can imagine a spectrum of intermediate growth conditions that would select for other taxa, irrespective of eddy age. Although protistan microzooplankton are known to graze heavily on diatoms under certain conditions, their implied ability to cause inefficient export from a substantial accumulated biomass of large diatoms deep in the euphotic zone was an unexpected outcome of this study. We advance strong grazing coupling as a hypothetical explanation for the low export measured from Cyclone *Opal*, but a full understanding of the fate of production in Cyclone *Opal* needs to account for the observed rates of population decline, measured growth rates and grazing contributions of micro- and mesozooplankton, direct sinking, and potential losses to lateral exchange.

Acknowledgments

This study was supported by NSF Grants 0241897 and 0324666 and by the Post-doctoral Fellowship Program of Korea Science & Engineering Foundation (KOSEF). We gratefully acknowledge the captain and crew of the R.V. *Wecoma*, and all of the E-Flux III shipmates and colleagues whose efforts facilitated and contributed to our results.

References

Allen, C.B., Kanda, J., Laws, E.A., 1996. New production and photosynthetic rates within and outside a cyclonic mesoscale eddy in the North Pacific Subtropical Gyre. Deep-Sea Research I 43, 917–936.

Benitez-Nelson, C., Bidigare, R.R., Dickey, T.D., Landry, M.R., Leonard, C.L., Brown, S.L., Nencioli, F., Rii, Y.M., Maiti, K., Becker, J.W., Bibby, T.S., Black, W., Cai, W.J., Carlson, C., Chen, F.Z., Kuwahara, V.S., Mahaffey, C., McAndrew, P.M., Quay, P.D., Rappé, M., Selph, K.E., Simmons, M.P., Yang, E.J., 2007. Mesoscale eddies drive increased silica export in the subtropical Pacific Ocean. Science 316, 1017–1021.

Bibby, T.S., Gorbunov, M.Y., Wyman, K.W., Falkowski, P.G., Brown, S.L., Rii, Y.M., Bidigare, R.R., 2008. Photosynthetic community responses to upwelling

mesoscale eddies in the subtropical north Atlantic and Pacific Oceans. Deep-Sea Research Part II, this volume [doi:10.1016/j.dsr2.2008.01.014].
Bidigare, R.R., Benitez-Nelson, C., Leonard, C.L., Quay, P.D., Parsons, M.L., Foley, D.G., Seki, M.P., 2003. Influence of a cyclonic eddy on microheterotroph biomass and carbon export in the lee of Hawaii. Geophysical Research Letters 30, 51–54.
Bidigare, R.R., Van Heukelem, L., Trees, C., 2005. Analysis of algal pigments by high-performance liquid chromatography. In: Andersen, R. (Ed.), Algal Culturing Techniques. Academic Press, New York, pp. 327–345.
Bidle, K.D., Azam, F., 1999. Accelerated dissolution of diatom silica by marine bacterial assemblages. Nature 397, 508–512.
Brown, S.L., Landry, M.R., Christensen, S., Garrison, D., Gowing, M.M., Bidigare, R.R., Campbell, L., 2002. Taxon-specific community dynamics and production in the Arabian Sea during the 1995 monsoon seasons. Deep-Sea Research II 49, 2345–2376.
Brown, S.L., Landry, M.R., Neveux, J., Dupouy, C., 2003. Microbial community abundance and biomass along a 180° transect in the equatorial Pacific during an El Niño-Southern Oscillation cold phase. Journal of Geophysical Research 108, 8139.
Brown, S.L., Landry, M.R., Selph, K.E., Yang, E.J., Rii, Y.M., Bidigare, R.R., 2008. Diatoms in the desert: plankton community response to a subtropical mesoscale eddy in the subtropical North Pacific. Deep-Sea Research Part II, this volume [doi:10.1016/j.dsr2.2008.02.012].
Brussard, C.P.D., Noordeloos, A.A.M., Riegman, R., 1997. Autolysis kinetics of the marine diatom *Ditylum brightwellii* (Bacillariophyceae) under nitrogen and phosphorus limitation. Journal of Phycology 33, 980–987.
Brzezinski, M.A., Nelson, D.M., Franck, V.M., Sigmon, D.E., 2001. Silicon dynamics within an intense open-ocean diatom bloom in the Pacific sector of the Southern Ocean. Deep-Sea Research II 48, 3997–4018.
Calbet, A., Landry, M.R., 2004. Phytoplankton growth, microzooplankton grazing and carbon cycling in marine systems. Limnology and Oceanography 49, 51–57.
Campbell, L., Vaulot, D., 1993. Photosynthetic picoplankton community structure in the subtropical North Pacific Ocean near Hawaii (station ALOHA). Deep-Sea Research Part I 40, 2043–2060.
Cavender-Bares, K.K., Mann, E.L., Chisholm, S.W., Ondrusek, M.E., Bidigare, R.R., 1999. Differential response of equatorial Pacific phytoplankton to iron fertilization. Limnology and Oceanography 44, 237–246.
Coale, K.H., Johnson, K.S., Fitzwater, S.E., Gordon, R.M., Tanner, S., Chavez, F.P., Ferioli, L., Sakamoto, C., Rogers, P., Millero, F., Steinberg, P., Nightingale, P., Cooper, D., Cochlan, W.P., Landry, M.R., Constantinou, J., Rollwagen, G., Trasvina, A., Kudela, R., 1996. A massive phytoplankton bloom induced by an ecosystem-scale iron fertilization experiment in the equatorial Pacific Ocean. Nature 383, 495–501.
De Baar, H.J.W., Boyd, P.W., Coale, K.H., Landry, M.R., Tsuda, A., Assmy, P., Bakker, D.C.E., Bozec, Y., Barber, R.T., Brzezinski, M.A., Buesseler, K.O., Boyé, M., Croot, P.L., Gervais, F., Gorbunov, M.Y., Harrison, P.J., Hiscock, W.T., Laan, P., Lancelot, C., Law, C.S., Levasseur, M., Marchetti, A., Millero, F.J., Nishioka, J., Nojiri, Y., van Oijen, T., Riebesell, U., Rijkenberg, M.J.A., Saito, H., Takeda, S., Timmermans, K.R., Veldhuis, M.J.W., Waite, A.M., Wong, C.-S., 2005. Synthesis of 8 iron fertilization experiments: from the iron age in the age of enlightenment. Journal of Geophysical Research 110, C09S16.
Dickey, T., Nencioli, F., Kuwahara, V., Leonard, C., Black, W., Bidigare, R., Rii, Y., Zhang, Q., 2008. Physical and bio-optical observations of oceanic cyclones west of the island of Hawaii. Deep-Sea Research Part II, this volume [doi:10.1016/j.dsr2.2008.01.006].
Eppley, R.W., Reid, F.M.H., Strickland, J.D.H., 1970. Estimates of phytoplankton crop size, growth rate, and primary production. In: Strickland, H.J.D. (Ed.), The Ecology of the Plankton off La Jolla California in the Period April through September 1967, vol. 17. Bull. Scripps Institution of Oceanography, pp. 33–42.
Froneman, P.W., Perissinotto, R., 1996. Structure and grazing of the microzooplankton communities of the Subtropical Convergence and a warm-core eddy in the Atlantic sector of the Southern Ocean. Marine Ecology Progress Series 135, 237–245.
Jacobson, D.M., Anderson, D.M., 1993. Growth and grazing rates of *Protoperidinium hirobis* Abè, a thecate heterotrophic dinoflagellate. Journal of Plankton Research 15, 723–736.
Jeong, H.J., Yoo, Y.D., Kim, E.T., Kang, N.S., 2004. Feeding by the heterotrophic dinoflagellate *Protoperidinium bipes* on the diatom *Skeletonema costatum*. Aquatic Microbial Ecology 36, 171–179.
Karl, D.M., Laws, E.A., Morris, P., Williams, P.J.L., Emerson, S., 2003. Metabolic balance of the open sea. Nature 426, 32.
Landry, M.R., Kirchman, D.L., 2002. Microbial community structure and variability in the tropical Pacific. Deep-Sea Research II 49, 2669–2694.
Landry, M.R., Haas, L.W., Fagerness, V.L., 1984. Dynamics of microplankton communities: experiments in Kaneohe Bay, Hawaii. Marine Ecology Progress Series 16, 127–133.
Landry, M.R., Brown, S.L., Campbell, L., Constantinou, J., Liu, H., 1998. Spatial patterns in phytoplankton growth and microzooplankton grazing in the Arabian Sea during monsoon forcing. Deep-Sea Research II 45, 2353–2368.
Landry, M.R., Ondrusek, M.E., Tanner, S.J., Brown, S.L., Constantinou, J., Bidigare, R.R., Coale, K.H., Fitzwater, S., 2000a. Biological response to iron fertilization in the eastern equatorial Pacific (IronEx II): I. Microplankton community abundances and biomass. Marine Ecology Progress Series 201, 27–42.
Landry, M.R., Constantinou, J., Latasa, M., Brown, S.L., Bidigare, R.R., Ondrusek, M.E., 2000b. Biological response to iron fertilization in the eastern equatorial Pacific (IronEx II). III: dynamics of phytoplankton growth and microzooplankton grazing. Marine Ecology Progress Series 201, 57–72.
Landry, M.R., Selph, K.E., Brown, S.L., Abbott, M.R., Measures, C.I., Vink, S., Allen, C.B., Calbet, A., Christensen, S., Nolla, H., 2002. Seasonal dynamics of phytoplankton in the Antarctic Polar Front region at 170°W. Deep-Sea Research II 49, 1843–1865.
Landry, M.R., Yang, E.J., Selph, K.E., Hodges, M., Bidigare, R.R., 2005. Depth-resolved microplankton dynamics in the equatorial Pacific. ASLO Meeting, Santiago de Compostela, Spain, June 2005.
Mann, E.L., Chisholm, S.W., 2000. Iron limits the cell division rate of *Prochlorococcus* in the Eastern Equatorial Pacific. Limnology and Oceanography 45, 1067–1076.
McGillicuddy Jr., D.J., Robinson, A.R., Siegel, D.A., Jannasch, H.W., Johnson, R., Dickey, T.D., McNeil, J., Michaels, A.F., Knap, A.H., 1998. Influence of mesoscale eddies on new production in the Sargasso Sea. Nature 394, 263–266.
McGillicuddy Jr., D.J., Johnson, R., Siegel, D.A., Michaels, A.F., Bates, N.R., Knap, A.H., 1999. Mesoscale variations of biogeochemical properties in the Sargasso Sea. Journal of Geophysical Research 104, 13381–13394.
Menden-Deuer, S., Lessard, E.J., 2000. Carbon to volume relationships for dinoflagellates, diatoms, and other protist plankton. Limnology and Oceanography 45, 569–579.
Michaels, A.F., Olson, D., Sarmiento, J.L., Ammerman, J.W., Fanning, K., Jahnke, R., Knap, A.H., Lipschultz, F., Prospero, J.M., 1996. Inputs, losses and transformations of nitrogen and phosphorus in the pelagic North Atlantic Ocean. Biogeochemistry 35, 181–226.
Monger, B.C., Landry, M.R., 1993. Flow cytometric analysis of marine bacteria with Hoechst 33342. Applied and Environmental Microbiology 59, 905–911.
Nencioli, F., Dickey, T.D., Kuwahara, V.S., Black, W., Rii, Y.M., Bidigare, R.R., 2008. Physical dynamics and biological implications of a mesoscale cyclonic eddy in the lee of Hawaii: Cyclone *Opal* observations during E-Flux III. Deep-Sea Research Part II, this volume [doi:10.1016/j.dsr2.2008.02.003].
Putt, M., Stoecker, D., 1989. An experimentally determined carbon:volume ratio for marine "oligotrichus" ciliates from estuarine and coastal waters. Limnology and Oceanography 34, 1097–1103.
Rii, Y.M., Brown, S.L., Nencioli, F., Kuwahara, V., Dickey, T., Karl, D.M., Bidigare, R.R., 2008. The transient oasis: nutrient–phytoplankton dynamics and particle export in Hawaiian lee cyclones. Deep-Sea Research Part II, this volume [doi:10.1016/j.dsr2.2008.01.013].
Sakamoto, C.M., Karl, D.M., Jannasch, H.W., Bidigare, R.R., Letelier, R.M., Walz, P.M., Ryan, J.P., Polito, P.S., Johnson, K.S., 2004. Influence of Rossby waves on nutrient dynamics and the plankton community structure in the North Pacific Subtropical Gyre. Journal of Geophysical Research 109, C05032.
Sarthou, G., Timmermans, K.R., Blain, S., Treguer, P., 2005. Growth physiology and fate of diatoms in the ocean: a review. Journal of Sea Research 53, 25–42.
Sherr, E.B., Sherr, B.F., 1993. Preservation and storage of samples for enumeration of heterotrophic protists. In: Kemp, P., Sherr, E., Sherr, B., Cole, J. (Eds.), Handbook of Methods in Aquatic Microbial Ecology. Lewis Publishers, Boca Raton, FL, pp. 207–212.
Siegel, D.A., McGillicuddy Jr., D.J., Fields, E.A., 1999. Mesoscale eddies, satellite altimetry, and new production in the Sargasso Sea. Journal of Geophysical Research 104, 13359–13379.
Sweeney, E.N., McGillicuddy, D.J., Buesseler, K.O., 2003. Biogeochemical impacts due to mesoscale eddy activity in the Sargasso Sea as measured at the Bermuda Atlantic Time-series Study (BATS). Deep-Sea Research Part II 50, 3017–3039.
Tarran, G.A., Zubkov, M.V., Sleigh, M.A., Burkill, P.H., Yallop, M., 2001. Microbial community structure and standing stocks in the NE Atlantic in June and July of 1996. Deep-Sea Research II 48, 963–985.
Tate, M.W., Clelland, R.C., 1957. Nonparametric and Shortcut Statistics in the Social, Biological, and Medical Sciences. Interstate Printers and Publishers, Inc., Danville, IL.
Vaillancourt, R.D., Marra, J., Seki, M.P., Parsons, M.L., Bidigare, R.R., 2003. Impact of a cyclonic eddy on phytoplankton community structure and photosynthetic competency in the subtropical North Pacific Ocean. Deep-Sea Research Part I 50, 829–847.
Verity, P., Langdon, C., 1984. Relationships between lorica volume, carbon, nitrogen, and ATP content of tintinnids in Narragansett Bay. Journal of Plankton Research 66, 859–868.
Yang, E.J., Choi, J.K., Hyun, J.-H., 2004. Distribution and structure of heterotrophic protist communities in the northeast equatorial Pacific Ocean. Marine Biology 146, 1–15.